B/CW/IN/31

2001 NASA/ASEE SUMMER FACULTY FELLOWSHIP PROGRAM

JOHN F. KENNEDY SPACE CENTER
UNIVERSITY OF CENTRAL FLORIDA

THERMAL DESIGN OF A COLLAPSIBLE CRYOGENIC VESSEL

Hisham E. Hegab, Ph.D., P.E.
Associate Professor
Mechanical Engineering Program
Louisiana Tech University
KSC Colleague - Michael Lonergan, P.E.
Spaceport Engineering & Technology Directorate

ABSTRACT

Strategic planning for human exploration missions to Mars has conclusively identified in-situ resource utilization (ISRU) as an enabling technology. Most mission scenarios include an ISRU plant to produce propellants for ascent from Mars as well as the production of backup reserves of water, oxygen, and process gases. Current mission scenarios call for an ISRU plant to be deployed and then produce and store the required propellants and life support reserves before the arrival of the first human mission. Reliable cryogenic propellant liquefaction and storage technologies for extended period missions are especially critical. This report examines the cryogenic storage problem for liquid oxygen produced by an ISRU plant for a human mission scenario. The analysis examines various hardware configurations including insulation types, packaging techniques, and required cryocoolers to minimize the initial launch mass to low Earth orbit. Results of the analyses indicate that high vacuum insulation systems requiring vacuum pressures below one millitorr will be required to minimize the initial launch mass into low Earth orbit even though the temperature on the surface of Mars is much lower than Earth.

THERMAL DESIGN OF A COLLAPSIBLE CRYOGENIC VESSEL

Hisham E. Hegab, Ph.D., P.E.

1. INTRODUCTION

The current NASA mission plan for the first hum mission to Mars is based on an in-situ resource utilization (ISRU) approach where propellants will be produced using a production plant on the surface of Mars for the return ascent from the surface. This approach reduces the amount of propellants needed to be taken to Mars and ultimately reduced the overall mission cost. Making propellants on Mars requires liquefaction, storage, and transfer of cryogens on Mars. Cryogenic propellant liquefaction and storage technologies for extended periods of operation are especially crucial to a successful mission scenario. The current baseline for a human mission calls for a 500- to 600-day period of operation for propellant production and at least 700-days of continued storage capability. Trade-off studies are underway to examine various possible mission approaches. This report examines the cryogenic liquefaction and storage problem for a human mission to mars and proposes hardware configurations for a collapsible storage tank to be used for liquid oxygen storage. A collapsible design is being investigated for possible volume and mass reductions in the total system mass that is launched from Earth into low Earth orbit. The scheme of using a collapsible tank design is a derivative of inflatable habitat structures that were proposed in previous updates of the human reference mission. The use of these inflatable structures resulted in significant mass reductions. The mission costs depend principally on the initial mass to low Earth orbit (IMLEO) and will not be feasible if it becomes excessive. Thus, the selected criterion for evaluating mission options is the minimization of the IMLEO. For this analysis, the total storage system mass includes the mass of the insulation and required cryocoolers.

2. ASSUMPTIONS AND THERMAL ENVIRONMENT

The cryogen storage options evaluated in this report are based upon the Reference Mission of the NASA Mars Exploration Study Team [1] and its updated addendum [2] as well as recent papers examining cryogenic system requirements for a Mars mission scenarios [3,4]. The reference mission has several key attributes, including short transits for humans to and from Mars with long surface stays, and rendezvous on the Martian surface. Transit times are planned at less than 180 days, with surface stays over 500 days. The reference mission overview consists of two cargo mission launches and one crew transit launch. The first cargo mission will transport the Earth return vehicle for the crew into Mars orbit, and the second cargo mission, launched at the same time as the first one, will consist of a cargo lander with the propellant production plant, power systems, human habitat, and ascent vehicle. Approximately 26 months after the initial cargo mission launches, a human crew insertion mission is launched. After completion of the 500-day surface mission, the crew ascends to Mars orbit and rendezvous with the pre-deployed Earth return vehicle.

After deployment of the cargo lander on the Mars surface, in situ propellant production of methane and oxygen will commence. Current mission scenarios call for the propellant production of approximately 30,000 kg of oxygen and 8,500 kg of methane for the ascent vehicle. In addition, 4,500 kg of oxygen needs to be produced as a life support cache while the human crew is at Mars. Additional oxygen will likely be needed for EVAs and rover surface excursions [2,5] from the surface habitat. Based upon this information, it was decided to develop conceptual designs for a storage tank that could handle 50,000 kg of liquid oxygen. For the initial analysis of the various insulation systems investigated, a cylindrical shape with spherical end caps was selected for the tank. To hold the required 50,000 kg of liquid oxygen,

a tank approximately 3-m in diameter and 4.5-m long (cylindrical section length) is required. It was assumed the outer surface of the tank would be coated with a reflective material to reduce solar absorption and maximize radiative surface emission. A solar absorptivity and surface emissivity of 0.15 and 0.85, respectively, were assumed for the surface of the tank. Aluminized films are commercially available that provide these radiative properties. Table 1 summarizes the assumed parameters of the storage tank.

For this analysis, a storage pressure of 27.6 kPa (4 psia) was selected for the liquid oxygen. This pressure was selected for a companion study examining concepts for the structural design of the collapsible tank. At this selected storage pressure, the corresponding saturation temperature of the liquid oxygen is approximately 79 K. Selecting a higher storage pressure of approximately 155 kPa (22.5 psia) can increase the storage temperature to approximately 95 K, but this change was determined to produce little effect on the required insulation. However, the increase in storage pressure produces more significant increases in the structural requirements of the vessel; thus, increasing its mass so it was determined the lower storage pressure was preferable. In addition, the density of the liquid oxygen is slightly greater at the lower storage pressure, which helps to reduce the required size of the storage vessel.

Table 1. Summary of assumed tank parameters

Parameter	Assumption
Shape	Cylindrical with spherical end caps
Diameter	3 m
Length	4.5 m
α_s	0.15
ε	0.85

Table 2 provides the environmental conditions that were used to analyze the heat leak to the storage vessel. These conditions are essentially the same as those used by Mueller and Durrant [6] for the analysis of propellant liquefaction and storage for a precursor mission to demonstrate the ISRU technology. Environmental conditions for a typical Martian day, night, and dust storm are examined. Fig. 1 illustrates the differences in solar irradiance between Earth and Mars as described by the Mars Reference Mission addendum [2]. Solar irradiation at the surface of Mars is significantly lower than that at Earth's surface and is strongly influenced by the presence of dust storms. Other sources of Mars environmental conditions were also examined [6,7] and the conditions listed in Table 2 were deemed reasonable design conditions for analyzing the vessel. It should be noted the conditions listed in Table 2 are nominal conditions and significant variations from them are possible depending upon the chosen landing site and variations in local weather conditions. Thus, an insulation system based upon these design conditions would be expected to occasionally encounter conditions beyond their limits and would require a pressure relief system to prevent structural damage to the vessel. In the absence of designated landing site for the reference mission, these environmental conditions should provide an adequate analysis for the current level of this feasibility study.

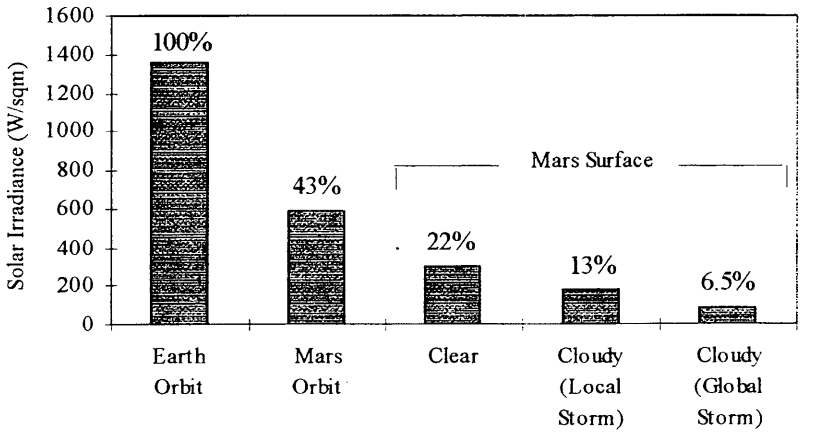

Figure 1. Earth and Mars solar irradiance comparison [2]

Table 2. Assumed Mars environment conditions

	Day	Night	Dust storm	Units
Average Solar irradiation	304	---	150	W/m^2
Atmosphere Temperature	230	190	210	K
Ground Temperature	220	195	200	K
Sky Temperature	170	130	200	K
Wind Speed	8	8	17	m/s

The insulation system design requirements are to obtain a near zero boil off rate for the stored liquid oxygen. To achieve this, cryocoolers will be required to re-liquefy any boil off from the storage tank due to heat leak. The additional mass of the cryocoolers is considered as part of the total insulation system mass but there is no mass penalty for the increased power needed for larger cryocoolers. For this analysis, it was assumed that the increase in cryocooler power requirements would have a negligible impact on the power system mass since the design reference mission calls for a nuclear power plant to support the human mission. Results from this study would need to be revised in the case of a solar power mission. The cryocooler efficiency was based upon the efficiency of a pulse tube cryocooler currently being developed for a Mars precursor mission [8]. This cryocooler is being specifically developed for liquefying oxygen on Mars and produces approximately 19 W of refrigeration for 222 W of input power ($COP_R = 0.086$). This performance is very high (~20% of Carnot efficiency) for a pulse tube cryocooler, but based upon the significant progress in improving cryocooler efficiencies in the last five years it is likely that cryocoolers used in a human mission to Mars would have similar or better efficiencies.

3. ANALYSIS APPROACH

Once the model assumptions and constraints were established, the analysis was developed to select the preferred insulation type, thickness required, and cryocooler capacity resulting in the minimum total insulation system mass (insulation mass + cryocooler mass + radiator mass). Several common cryogenic insulation types were considered including multilayer insulation (MLI), aerogel blankets, microspheres, opacified powder, perlite, and a new layered composite insulation (LCI) being developed at KSC. These various insulation types were evaluated at various ranges of ambient pressure ranging from high vacuum (<0.001 torr) to the atmospheric pressure on Mars (~7 torr). The apparent thermal conductivities and densities of the various insulation types at their respective pressures are provided in Table 3.

In order to estimate the insulation thickness and cryocooler capacity required an energy balance was conducted at the tank surface, which includes solar irradiance, radiation exchange with the environment, convection with the atmosphere, and conduction through the insulation as shown in Fig. 2. A simple one-dimensional, steady state heat transfer analysis was used. For simplicity, the tank was assumed to be cylindrical with spherical end caps. The structural design may require more of an egg shape to provide support to hold the weight of the liquid oxygen but would not significantly affect the results of this analysis.

Table 3. Insulation types examined

Insulation	Apparent k (mW/m-K)	Density (kg/m^3)	Vacuum Level*
MLI [9]	0.08	58	High
	2.68	58	Soft
Aerogel blanket [9]	0.55	125	High
	1.16	125	Soft
	4.97	125	Ambient
Layered Composite Insulation [9]	0.09	52	High
	1.23	52	Soft
	5.56	52	Ambient
Microspheres [10]	0.39	130	High
Opacified powder [10]	0.48	80	High
Perlite [11]	1.10	135	High
	2.50	135	Soft

* high vacuum ≈ 0.001 torr or less, soft vacuum ≈ 0.1 torr, ambient ≈ 7 torr

A model of the tank using three nodes to represent the surface temperature of the tank on the top hemisphere, the cylindrical side, and the bottom hemisphere was developed. Each surface node allows for convection and radiation to the atmosphere and absorption of direct solar irradiation. The three surface nodes are also linked to a single fixed temperature node representing the liquid oxygen temperature.

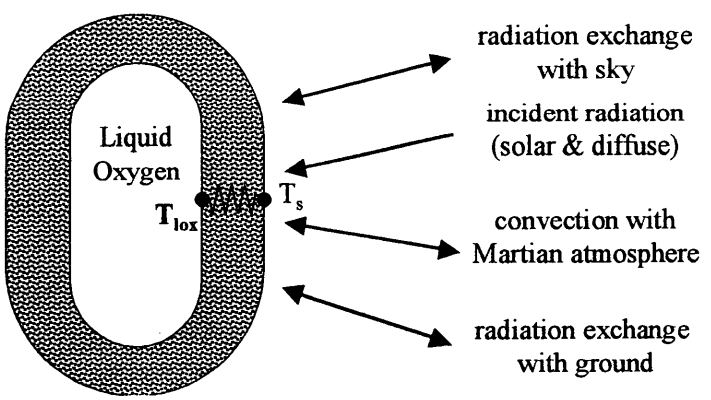

Figure 2. Energy balance schematic

In the following equations, the insulation properties (thermal conductivity and density) and boil off rate of the liquid oxygen are the inputs, and the desired outputs are the insulation system masses as well as other operating parameters such as tank surface temperature, heat leak, cryocooler power, etc.

$$\frac{T_{surf,i}-T_{lox}}{R_{ins,i}} = q_{solar,i} + \frac{T_{atm}-T_{surf,i}}{R_{conv,i}} + \frac{J_{surf,i}-\sigma T_{surf,i}^4}{\frac{1-\varepsilon}{\varepsilon A_i}} \quad \text{where} \quad i = 1\ldots3 \tag{1}$$

$$\frac{J_{surf,i}-\sigma T_{surf,i}^4}{\frac{1-\varepsilon}{\varepsilon A_i}} = \frac{\sigma T_{sky}^4 - J_{surf,i}}{\frac{1}{A_i F_{i3}}} + \frac{\sigma T_g^4 - J_{surf,i}}{\frac{1}{A F_{i2}}} \quad \text{where} \quad i = 1\ldots3 \tag{2}$$

$$R_{ins,1} = \frac{\ln\left[\frac{D/2 + t_{ins}}{D/2}\right]}{2\pi k_{ins} L} \quad R_{ins,2,3} = \frac{\frac{1}{D/2} - \frac{1}{D/2 + t_{ins}}}{4\pi k_{ins}} \quad R_{conv,i} = \frac{1}{h_{c,i} A_i} \quad \text{where } i = 1\ldots3 \tag{3}$$

$$q_{solar,1} = \alpha_s \frac{A_1}{2} \quad q_{solar,2} = \alpha_s A_2 \quad q_{solar,3} = 0 \tag{4}$$

$$q_{leak} = \frac{T_{surf,1}-T_{lox}}{R_{ins,1}} + \frac{T_{surf,2}-T_{lox}}{R_{ins,2}} + \frac{T_{surf,3}-T_{lox}}{R_{ins,3}} \tag{5}$$

$$\dot{m}_{boiloff} = \frac{q_{leak}}{h_{fg}} \tag{6}$$

$$m_{insulation} = \rho_{ins} t_{ins} A \tag{7}$$

$$m_{cryocooler} = 0.9 \cdot \frac{171.85}{(T_{lox}-10)^{0.85}} \cdot q_{leak} \tag{8}$$

$$m_{radiator} = 0.05 P_{cryocooler} \tag{9}$$

$$P_{cryocooler} = \frac{q_{leak}}{0.2[T_{atm} - (T_{lox}-10)]} \tag{10}$$

$$m_{total} = m_{insulation} + m_{cryocooler} + m_{rad} \tag{11}$$

Eqs. (1) and (2) are energy balances at the tank surface for each of the three nodes. Variables for the three surface nodes are denoted by the subscript i, where $i = 1$ corresponds to the cylindrical side of the vessel, $i = 2$ corresponds to the top hemispherical cap, and $i = 3$ corresponds to the bottom hemispherical cap. The unknowns determined by these equations are the tank surface temperatures, $T_{surf,i}$, and the tank surface radiosities, $J_{surf,i}$. The insulation thermal resistance, $R_{ins,i}$, and convection thermal resistance, $R_{conv,i}$, in Eq. (1) are determined by Eq. (3) using one dimensional, steady state heat transfer equations. The convection coefficients, $h_{c,i}$, were determined using a Nusselt number correlations by Churchill and Bernstein for a cylinder in crossflow [12] and by Whitaker [12] for flow over a sphere for the selected atmospheric conditions. The view factors, F_{12} and F_{13}, are from the tank cylindrical surface to the ground and to the sky, respectively. They were determined using the geometry of the tank assuming no interference from other deployed equipment and both found to be 0.5 [13]. The top hemisphere node only exchanges radiation with the sky and similarly the bottom hemisphere node only exchanges radiation with the ground. Consequently, view factors F_{22} and F_{33} are zero and view factors F_{23} and F_{32} are one. The solar

irradiation for each surface node was determined using Eq. (4). It is assumed that half of the tank is exposed to the influx of solar irradiation such that the half of the cylindrical side surface area and the entire top hemispherical cap area are exposed. The heat leak, q_{leak}, into the liquid oxygen is calculated by Eq. (5). The boil off rate of the liquid oxygen is determined by Eq. (6), where the heat of vaporization, h_{fg}, was determined from the saturation pressure of the liquid oxygen. The individual insulation system masses are determined in Eqs. (7) – (9). Eq. (8) is an empirical correlation developed by Kittel et al. [4] that predicts cryocooler mass based upon commercially available cryocoolers. Eq. (9) is another empirical correlation that predicts the required radiator mass for the cryocooler [6]. Eq. (10) is used to estimate the cryocooler power assuming that it has a 20% Carnot efficiency [8]. Finally, the total insulation system mass is determined by Eq. (11).

4. RESULTS AND DISCUSSION

The results of the optimization of the various insulation systems for the nominal day environmental conditions are shown in Figs. 3 and 4. In Fig 3., the total insulation system mass is shown as a function of boil off rate of the liquid oxygen for the various insulation systems. In Fig. 4, the total insulation system mass is shown as a function of the insulation thickness. As expected, there is an optimal tradeoff between insulation mass and cryocooler mass. As the system insulation mass increases, the required cooler capacity, and consequently mass, decreases. Table 4 provides a summary of system parameters that minimize the total insulation system mass for each of the insulations for a nominal daytime environment on Mars. From examining the results, it is apparent that the high vacuum MLI and LCI systems provide the smallest total insulation system mass. Each offers almost the same IMLEO for the same insulating performance. It is also noted that the outer surface temperature of a well-insulated tank is essentially independent of the insulation type used and primarily depends on the external environment conditions and tank surface radiative properties. There is approximately an order of magnitude penalty in the total insulation system mass for using soft vacuum insulation systems compared to the high vacuum MLI and LCI. Soft vacuum or ambient pressure insulation systems would be desirable for their greater reliability and simplicity but would not likely be the best choice because of the significant mass penalty.

Table 4. Insulation system parameters for minimal IMLEO

Insulation	Vacuum level*	t_{ins} (cm)	Q_{leak} (W)	T_{surf} (K)	$P_{cryocooler}$ (W)	$m_{insulation}$ (kg)	$m_{cryocooler}+m_{rad}$ (kg)	m_{total} (kg)
MLI	High	3.6	31.1	217	361	146.3	149.2	295.6
	Soft	20.5	195.8	216	2267	840.6	937.9	1778.5
Aerogel blanket	High	6.3	121.6	216	1408	560.8	582.6	1142.4
	Soft	9.2	179.1	216	2075	812.3	858.2	1670.5
	Ambient	18.8	388.4	214	4498	1665.0	1861.0	3526.0
LCI	High	4.0	31.3	217	363	146.9	150.2	297.1
	Soft	14.7	122.2	216	1415	541.0	585.5	1126.5
	Ambient	31.0	280.0	215	3243	1142.0	1342.0	2484.0
Microspheres	High	5.2	103.9	216	1203	482.0	497.6	979.6
Opacified powder	High	7.4	91.4	216	1058	419.8	437.8	857.6
Perlite	High	8.6	180.8	216	2093	822.0	866.0	1688.0
	Soft	12.9	278.3	215	3223	1233.0	1333.0	2566.0

* high vacuum ≈ 0.001 torr or less, soft vacuum ≈ 0.1 torr, ambient ≈ 7 torr

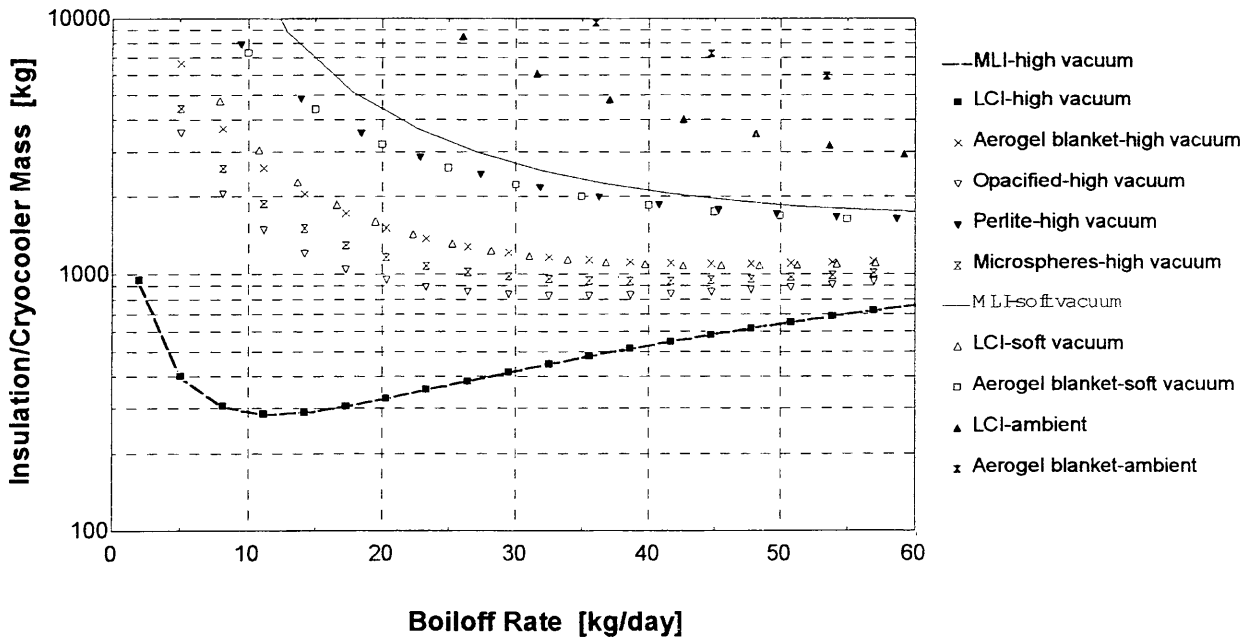

Figure 3. Insulation system mass versus boil off rates for nominal Martian day

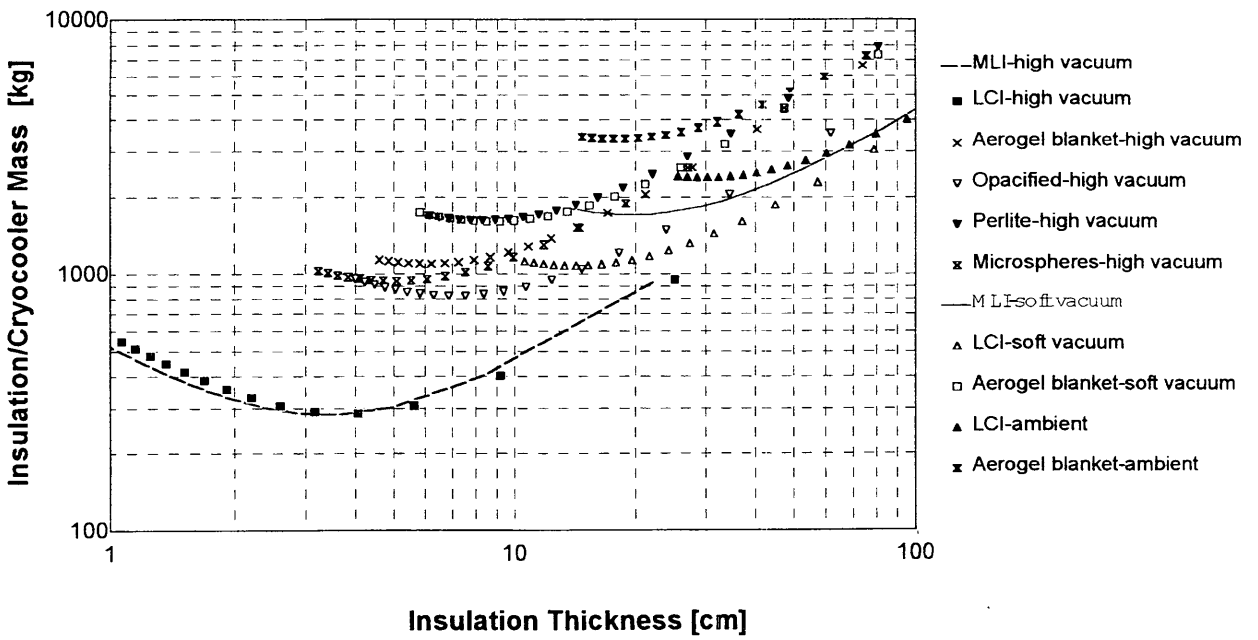

Figure 4. Insulation system mass as function of insulation thickness for nominal Martian day

Table 5 summarizes the operating conditions of the two insulation types with the lowest IMLEO, high vacuum MLI and LCI, for the three assumed nominal environmental conditions. Both insulations perform essentially the same since they have almost the same densities and thermal conductivities. Consequently, other factors such as reliability, installation, and packaging should be considered when selecting between the two. For a collapsible storage vessel design, reliability and packaging issues would likely be disadvantages for using MLI. MLI is highly anisotropic so its performance can be severely degraded by edge effects in its installation. In addition, its thermal performance is easily degraded by compression loading effects, which are a likely loading condition for a collapsible structure since a rigid

outer vessel wall is not desirable in a collapsible design. While it is anticipated that the layered composite insulation would be susceptible to these disadvantages as well it is difficult to calculate approximately how it would perform because of the lack of experimental data on it. Thermal performance under slight compressive loads is needed as well as experiments on edge effects associated with packaging it in vacuum-sealed polymer sheets.

Table 5. Summary of operating conditions for high vacuum MLI and LCI

Parameter	3.6 cm of MLI-high vacuum			4.0 cm of LCI-high vacuum		
	Day	Night	Dust storm	Day	Night	Dust storm
Q_{leak} (W)	31.1	22.2	29.1	31.4	22.3	29.3
$m_{boiloff}$ (kg/day)	12.1	8.6	11.3	12.1	8.6	11.4
T_{surf} (K)	217	177	208	217	177	208

Packaging of any selected insulation type is a significant issue for a collapsible design. It is envisioned that vacuum insulation panel technologies would be used for packaging LCI or MLI. Typical vacuum insulation panels consist of three components as shown in Fig. 5. The core material is the selected insulation such as LCI. The barrier/envelope may consist of a metal foil or polymer and serves to protect the insulation from permeation and possibly as a radiative shield. The most suitable choice for this application would most likely be a polymer with thin layer of metal vapor deposited on it. Using metal foils for the barrier provides a heat conduction path around the insulation so very thin layers are required to limit the heat leak. Getters and desiccants are typically used to maintain the vacuum level in the insulation panel. There are a number of commercial developers of this technology and vacuum levels below 0.003 torr have been maintained for more than two years in laboratory testing. Selection and design of the envelope, getters, and desiccants is a complicated matter and must be matched to the selected insulation as well as the external operating environment and desired vacuum level. Further studies on designing a vacuum insulation package for this application would be needed to be able to predict heat leaks due to edge effects as well as predict the thermal performance of the system over an extended period of operation.

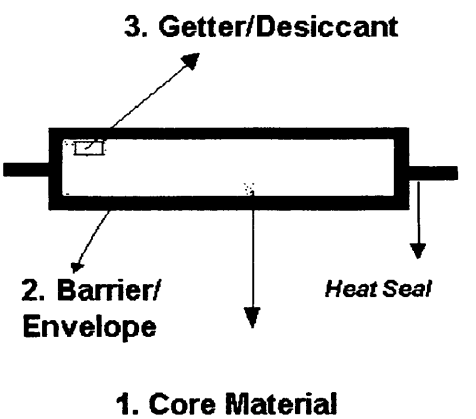

Figure 5. Components of a vacuum insulation panel

5. CONCLUSIONS

Based upon the analysis results, the surface temperature of a cryogenic storage vessel on Mars is primarily determined by solar irradiation, surface radiative properties, and convection with the atmosphere. For a properly insulated tank, the surface temperature of the tank is essentially independent of the insulation selected. The optimal insulation systems that minimize the initial launch mass to low Earth orbit are high vacuum systems using MLI or a layered composite insulation being developed at KSC. These insulations combined with a cryocooler system could achieve near zero boil-off rates with a total insulation system mass of approximately 300 kg. The corresponding heat leak into the storage tank and required cryocooler power are approximately 30 W and 360 W, respectively. The analysis assumes that there is no mass penalty for the cryocooler power. A solar powered human mission scenario would present significant complications to the cryogenic liquefaction and storage problem and may produce different results for the optimal insulation parameters. Vacuum insulation panel technology could be used to develop a packaging system for the insulation such that it could be integrated into a collapsible design, but the design of such a system would need to be tailored to the expected environmental conditions on Mars.

ACKNOWLEDGEMENTS

I would like to express my sincere appreciation to my NASA-KSC colleague Mike Lonergan for sponsoring me on this project. I would also like to thank Ray Hosler, Cassie Spears, and Greg Buckingham for their efforts in supporting the Summer Faculty Fellowship Program at KSC. Many thanks to everyone who helped to make this summer an enjoyable and interesting experience.

REFERENCES

[1] Hoffman, S. J., Kaplan, D. I., editors, Human Exploration of Mars: The Reference Mission of the NASA Mars Exploration Study Team, Johnson Space Center, July 1997.

[2] Drake, B., editor, Reference Mission 3.0 Addendum to the Human Exploration of Mars: The Reference Mission of the NASA Mars Exploration Study Team, Johnson Space Center, June, 1998.

[3] Salerno, L. J., and Kittel, P., Cryogenics and the human exploration of Mars, *Cryogenics*, 39, 1999, p. 381-388.

[4] Kittel, P., Salerno, L. J., and Plachta, D.W., Cryocoolers for Human and Robotic Missions to Mars, *Cryocoolers 10*, Kluwer Academic/Plenum Publishers, 1999, pp. 815-821.

[5] Sridhar, K. R., Finn, J. E., and Kliss, M. H., In-Situ Resource Utilization Technologies for Mars Life Support Systems, *Adv. Space Res.*, vol. 25, no. 2, 2000, pp 249-255.

[6] Mueller, P., and Durrant, T., Cryogenic propellant liquefaction and storage for a precursor to a human Mars mission, *Cryogenics*, 39, 1999, pp. 1021-1028.

[7] Environment of Mars, NASA-TM 100470, October 1988.

[8] Marquardt, E. D., Radebaugh, R., Pulse Tube Oxygen Liquefier, *Adv. Cryogenic Engineering*, vol. 45, 2000, pp. 457-464.

[9] Augustynowicz, S. D., and Fesmire, J. E., Cryogenic Insulation System for Soft Vacuum, KSC-00408 Report, 1999, pp. 1-7.

[10] Barron, R. F., *Cryogenic Systems, 2nd Ed.*, 1985, pp. 391-396.

[11] Barron, R. F., Cryogenic Heat Transfer, 1999, pp. 29-33.

[12] Incropera, F. P. and DeWitt, D. P., *Introduction to Heat Transfer, 3rd Ed.*, 1996, p. 345-349.

[13] Rea, S. N., Rapid Method for Determining Concentric Cylinder Radiation View Factors, *AIAA Journal*, 13, 8, August 1975, pp. 1122-1123.